Loss of translation elongation factor (eEF1A2) expression in vivo differentiates between Wallerian degeneration and dying-back neuronal pathology

Journal of Anatomy

J. Anat. (2008) **213**, pp633–645 doi: 10.1111/j.1469-7580.2008.01007.x

Loss of translation elongation factor (*eEF1A2*) expression *in vivo* differentiates between Wallerian degeneration and dying-back neuronal pathology

Lyndsay M. Murray,[1,2] Derek Thomson,[1,2] Annalijn Conklin,[1,2] Thomas M. Wishart[1,2] and Thomas H. Gillingwater[1,2]

[1]*Centre for Integrative Physiology and*
[2]*Centre for Neuroscience Research, College of Medicine and Veterinary Medicine, University of Edinburgh, Edinburgh EH8 9XD, UK*

Abstract

Wallerian degeneration and dying-back pathology are two well-known cellular pathways capable of regulating the breakdown and loss of axonal and synaptic compartments of neurons *in vivo*. However, the underlying mechanisms and molecular triggers of these pathways remain elusive. Here, we show that loss of translation elongation factor *eEF1A2* expression in lower motor neurons and skeletal muscle fibres in homozygous *Wasted* mice triggered a dying-back neuropathy. Synaptic loss at the neuromuscular junction occurred in advance of axonal pathology and by a mechanism morphologically distinct from Wallerian degeneration. Dying-back pathology in *Wasted* mice was accompanied by reduced expression levels of the zinc finger protein ZPR1, as found in other dying-back neuropathies such as spinal muscular atrophy. Surprisingly, experimental nerve lesion revealed that Wallerian degeneration was significantly delayed in homozygous *Wasted* mice; morphological assessment revealed that ~80% of neuromuscular junctions in deep lumbrical muscles at 24 h and ~50% at 48 h had retained motor nerve terminals following tibial nerve lesion. This was in contrast to wild-type and heterozygous *Wasted* mice where < 5% of neuromuscular junctions had retained motor nerve terminals at 24 h post-lesion. These data show that *eEF1A2* expression is required to prevent the initiation of dying-back pathology at the neuromuscular junction *in vivo*. In contrast, loss of *eEF1A2* expression significantly inhibited the initiation and progression of Wallerian degeneration *in vivo*. We conclude that loss of *eEF1A2* expression distinguishes mechanisms underlying dying-back pathology from those responsible for Wallerian degeneration *in vivo* and suggest that *eEF1A2*-dependent cascades may provide novel molecular targets to manipulate neurodegenerative pathways in lower motor neurons.

Key words axon; neuromuscular junction; neuropathology; synapse; *Wasted* mice.

Introduction

Pathways regulating neuronal vulnerability *in vivo* are of critical importance to our understanding of a wide spectrum of neurodegenerative disorders from Alzheimer's disease to motor neuron disease. A significant body of evidence now suggests that the maintenance of neuronal viability is compartmentalized within neurons, as cell soma, axons and synapses are all capable of independent regulation. One significant consequence of this compartmentalization is that distal neuronal compartments such as axons and synapses are particularly sensitive to perturbations of neuronal homeostasis (Gillingwater & Ribchester, 2001; Coleman, 2005; Gillingwater et al. 2006; Wishart et al. 2006; Bettini et al. 2007; Saxena & Caroni, 2007; Baxter et al. 2008).

Several apparently distinct cellular pathways are known to be capable of bringing about the degeneration of axons and synaptic terminals, including dying-back pathology and Wallerian degeneration (WD). For example, several different motor neuron diseases and sensory neuropathies are thought to occur primarily via dying-back pathways (Schmalbruch et al. 1991; Frey et al. 2000; Cifuentes-Diaz et al. 2002; Fischer et al. 2004; Keswani et al. 2006; Murray et al. 2008), whereas conditions such as multiple sclerosis and degeneration after traumatic nerve injury are more commonly associated with WD (Ferguson et al. 1997; Perry & Anthony, 1999; Gillingwater & Ribchester, 2001). Morphologically, WD is characterized by rapid axonal and synaptic fragmentation associated with disruption and loss of organelles and plasma membranes, breakdown of the axonal myelin sheath, and phagocytosis of synaptic and axonal debris by cells including Schwann cells and invading macrophages (for review see Gillingwater & Ribchester, 2001). At the

Correspondence
Thomas H. Gillingwater, Centre for Integrative Physiology, University of Edinburgh Medical School, Edinburgh EH8 9XD, UK.
T: +44 (0)131 6503724; E: t.gillingwater@ed.ac.uk

Accepted for publication *23 September 2008*

neuromuscular junction (NMJ), this process is characterized by an early depletion of synaptic vesicles, swollen and burst mitochondria, a breakdown of pre-synaptic plasma membranes and terminal Schwann cell processes penetrating into the synaptic cleft (Miledi & Slater, 1970; Winlow & Usherwood, 1975; Gillingwater et al. 2003). By contrast, dying-back neuropathies are characterized by a wave of degeneration beginning at, and progressing retrogradely from, the distal extremities of the neuron. Here, the early withdrawal/retraction of synaptic terminals at the NMJ occurs via a process devoid of the gross fragmentation associated with WD and more akin to a progressive reabsorption of synaptic and distal axonal organelles and plasma membranes back into the parent axon (for review see Gillingwater & Ribchester, 2003). Despite these clear morphological differences little is known about the extent to which their underling molecular mechanisms converge or diverge (Coleman, 2005; Hoopfer et al. 2006). However, evidence has been presented suggesting that morphologically distinct degeneration pathways can share common mechanistic links (Coleman, 2005; Mi et al. 2005). More detailed knowledge of the cellular and molecular mechanisms that regulate and perturb viability in distal neuronal compartments is therefore of significant importance for our understanding of the healthy and pathological nervous system.

Here, we detail neuropathological changes occurring in the peripheral nervous system of mice carrying a spontaneous mutation that abolishes the expression of a gene encoding the translation elongation factor *eEF1A2* [*Wasted* (*Wst*); Shultz et al. 1982; Chambers et al. 1998]. *eEF1A* (of which there are two variant forms, i.e. *eEF1A1* and *eEF1A2*) is the second most abundant protein in non-proliferating cells, constituting 1–2% of total protein and playing an integral role in the elongation stages of protein synthesis during which the polypeptide chain is assembled (Condeelis, 1995). Alongside important roles in protein synthesis, eEF1A proteins have also been postulated to have roles in non-canonical pathways including modification of the cytoskeleton (Condeelis, 1995), the heat shock response (Shamovsky et al. 2006) and synaptic plasticity (Giustetto et al. 2003). Expression patterns of the two variant forms (*eEF1A1* and *eEF1A2*) are mutually exclusive in all cells and tissues examined. The *eEF1A2* variant is only expressed in mature, terminally differentiated neurons and muscle (Pan et al. 2004). Its post-natal appearance in nerve and muscle coincides with loss of *eEF1A1* expression. *eEF1A1* is expressed ubiquitously at the time of birth but its expression in nerve and muscle declines from the first post-natal week onwards, being absent by post-natal day (P)20–21 (Pan et al. 2004). During this period of declining *eEF1A1* expression in nerve and muscle, its role is normally replaced by correlated increasing expression levels of *eEF1A2* (Chambers et al. 1998; Khalyfa et al. 2001), with the latter being the sole translation elongation factor by P21.

It has previously been shown that loss of *eEF1A2* results in the degeneration of lower motor neurons in *Wst* mice, characterized by vacuolation and neurofilament accumulation in neuronal soma and denervation of skeletal muscle fibres (Newbery et al. 2005). Importantly, the onset of degeneration correlates precisely with the switch to reliance on *eEF1A2* expression (Newbery et al. 2005) and it has been conclusively demonstrated that the specific loss of *eEF1A2* function is solely responsible for these events (Newbery et al. 2007). Preliminary observations of the morphological correlates of degeneration at the NMJ in homozygous *Wst* mice (Newbery et al. 2005) highlighted potential similarities to neuropathological events previously described in other mouse models of dying-back neuropathy (e.g. Frey et al. 2000; Cifuentes-Diaz et al. 2002; Fischer et al. 2004; Murray et al. 2008). However, dying-back pathways were not conclusively demonstrated in this study (Newbery et al. 2005). We have therefore undertaken a detailed qualitative and quantitative analysis of synaptic and axonal pathology in *Wst* mice to determine whether dying-back pathways are indeed instigated following the loss of *eEF1A2* expression *in vivo*. We show that the absence of normal post-natal *eEF1A2* expression in *Wst* mice leads to early-onset degeneration of motor nerve terminals, resulting in a dying-back pathology distinct from classic WD. Quantitative protein expression experiments showed that dying-back pathology in *Wst* mice correlated with reductions in expression levels of the zinc finger protein ZPR1. Surprisingly, a parallel set of nerve lesion experiments in homozygous *Wst* mice revealed delayed WD of distal axons and synaptic terminals, demonstrating that *eEF1A2* is required for the normal initiation and progression of WD pathways. These experiments demonstrate that loss of *eEF1A2* expression distinguishes mechanisms underlying dying-back pathways from those responsible for WD *in vivo*.

Materials and methods

Mouse maintenance and surgery

Pairs of heterozygous *Wst* mice were kindly provided by Dr Cathy Abbott (University of Edinburgh) and a breeding colony established. Litters contained homozygous and heterozygous mice as well as wild-type littermates. Heterozygous and wild-type littermates were used throughout as controls. Breeding colonies of *YFP-H* mice (Feng et al. 2000) were already established in animal care facilities at the University of Edinburgh and were crossed with *Wst* mice in order to obtain homozygous and heterozygous *Wst* mice, as well as wild-type littermates, endogenously expressing yellow fluorescent protein (YFP) in a subset of neurons. *Smn–/–;SMN2* mice (Monani et al. 2000) were obtained from existing breeding colonies in Edinburgh. All mice were housed in a semi-barrier facility and were fed a standard chow diet. *Wst*, *Wst;YFP-H* and *Smn–/–;SMN2* mice were genotyped using standard polymerase chain reaction techniques, as described previously (Newbery et al. 2005; Murray et al. 2008). The *YFP* status was ascertained by examining ear punches for evidence of YFP-labelled neurons. Mice were killed by overdose of isofluorane via

inhalation or cervical dislocation. *Wst* mice and wild-type littermates were killed at P20 for early-symptomatic data and P24–P27 for late-symptomatic data. All surgical procedures were performed under general anaesthesia (inhalation of isofluorane; 2% in 1:1 N_2O/O_2) as described previously (Gillingwater et al. 2003). All breeding and surgical procedures were carried out with the licensed authority of the UK Home Office.

Immunohistochemistry

Muscles were immunohistochemically labelled to allow quantification of neuromuscular innervation as described previously (Murray et al. 2008). Briefly, muscles were immediately dissected from recently killed mice and dissected in oxygenated mammalian physiological saline before labelling post-synaptic acetylcholine receptors with α-bungarotoxin conjugated to tetramethylrhodamine isothiocyanate (5 μg mL^{-1} for 10 min, Molecular Probes, USA). Muscles were then fixed in 4% paraformaldehyde in phosphate-buffered saline (PBS) for 1–2 h. Non-YFP-expressing muscles were then blocked in 4% bovine serum albumin and 1% TritonX in 0.1 M PBS for 30 min before incubation overnight in primary antibodies raised against either 165 kDa neurofilament proteins and the synaptic vesicle protein SV2 (both 1:200, Developmental Studies Hybridoma Bank, USA) or 150 kDa neurofilament proteins (Chemicon, USA) and visualized with sheep anti-mouse fluorescein isothiocyanate-conjugated secondary antibodies (1:200; Diagnostics Scotland, UK) or swine anti-rabbit fluorescein isothiocyanate-conjugated secondary antibodies (1:40; DAKO, USA), respectively. Muscles were then whole-mounted in Mowoil® (Calbiochem) on glass slides and coverslipped for subsequent imaging.

FM4–64FX labelling of neuromuscular synaptic function

Freshly dissected levator auris longus (LAL) muscles from *Wst;YFP-H* mice were loaded with the styryl dye FM4–64FX using a high K^+ stimulus. Muscle preparations were exposed to a fixable form of the styryl dye FM4–64 (FM4–64FX, 2 mg mL^{-1}; Molecular Probes) in high K^+ Krebs' solution sparged with 95% : 5% O_2 : CO_2 (102 mM Na^+, 50 mM K^+, 2 mM Ca^{2+}, 2 mM Mg^{2+}, 132 mM Cl^-, 23.8 mM HCO_{3-}, 0.4 mM $H_2PO_4^{2-}$, 5 mM D-glucose, 5.5 mM HEPES, pH 7.2–7.4) for 10 min. After rigorous washing, muscles were fixed in 4% paraformaldehyde/PBS solution (Electron Microscopy Science, PA, USA) and post-synaptic acetylcholine receptors were labelled with α-bungarotoxin conjugated to alexa-647 (5 μg mL^{-1} for 10 min, Invitrogen, USA). Muscles were whole-mounted in Mowoil® (Calbiochem) on glass slides and coverslipped for subsequent imaging.

Imaging and quantification

Immunohistochemically-labelled NMJs and YFP-expressing muscles and nerves were imaged using either a standard epifluorescence microscope equipped with a chilled charge-coupled device camera (40× objective; 0.8 NA; Nikon IX71 microscope; Hammamatsu C4742-95; Improvision Openlab Software) or a laser scanning confocal microscope (40× objective; 0.8 NA; Radiance 2000, Biorad, Hemel Hempstead, UK; Biorad Lasersharp 2000 Software). Between 50 and 200 endplates, selected at random, were quantified from each muscle preparation. Wherever possible, all analysis was performed without the operator knowing the status of the material. For basic occupancy counts, the occupancy of individual NMJs was evaluated by categorizing endplates as either fully occupied (neurofilament/SV2 entirely overlies endplate), partially occupied (neurofilament/SV2 partially covers endplate) or vacant (no neurofilament/SV2 overlies endplate).

Montages and reconstructions

Reconstructions of immunohistochemically-labelled and YFP-H-labelled muscle and nerve preparations were produced using Adobe Photoshop software by layering and combining multiple individual micrographs.

Electron microscopy

Nerve and muscle preparations were prepared for electron microscopy as described previously (Gillingwater et al. 2003). Briefly, preparations were fixed in 0.1 M phosphate buffer containing 4% paraformaldehyde and 2.5% glutaraldehyde for 4 h before post-fixation in 1% osmium tetroxide for 45 min. Following dehydration and propylene oxide stages, preparations were embedded in Durcupan resin. Ultra-thin sections (75–90 nm) were cut and collected on formvar-coated grids (Agar Scientific, UK), stained with uranyl acetate and lead citrate in an 'Ultrostainer' (LKB), and then viewed in a transmission electron microscope (CM12, Philips). Synaptic vesicle densities were calculated as described previously (Gillingwater et al. 2003).

Quantitative fluorescent (Li-COR) western blots

Total protein was isolated from the spinal cord of late-symptomatic *Wst* mice and control littermates as well as late-symptomatic (P5/P6) *Smn–/–;SMN2* mice and control littermates ($N = 3$ mice per genotype; see Murray et al. 2008) and quantitative western blots were performed as described previously (Wishart et al. 2007). Briefly, protein was separated by sodium dodecyl sulphate-polyacrylamide gel electrophoresis on 4–20% pre-cast NuPage 4–12% Bis Tris gradient gels (Invitrogen) and then transferred to a polyvinylidene difluoride membrane overnight. The membranes were blocked using Odyssey blocking buffer (Li-COR Biosciences) and incubated with primary antibodies as per the manufacturer's instructions (tubulin, Abcam; SMN1, BD Bioscience; ZPR1, BD Bioscience). Odyssey secondary antibodies were added according to the manufacturer's instructions (goat anti-rabbit IRDye 680 and goat anti-mouse IRDye 800). Blots were imaged using an Odyssey Infrared Imaging System (Li-COR Biosciences). The scan resolution of the instrument ranged from 21 to 339 μm and in this study blots were imaged at 169 μm. Quantification was performed on single channels with the analysis software provided. Bands were identified according to their relative molecular weight and delineated using Odyssey software and the arbitrary fluorescence intensity calculated by the software. For each membrane, scans were carried out at three different intensities in order to minimize possible user error in determining correct scan intensities or oversaturation of the membrane. The average of these three separate scans (giving an $N = 1$ per membrane) was used for analysis.

Results

Loss of *eEF1A2* expression triggers a dying-back neuropathy: synaptic pathology

In order to investigate the cellular pathway(s) through which lower motor neurons degenerate following perturbations

in expression of the translation elongation factor *eEF1A2* in *Wst* mice, we used confocal and electron microscopy to examine the detailed morphological correlates of neuromuscular pathology in two muscle groups previously shown to be affected in *Wst* mice, i.e. transversus abdominis from the anterior abdominal wall and deep lumbrical muscles from the hind-paw (Newbery et al. 2005). In both of these muscle groups, immunohistochemical labelling of distal axons and pre-synaptic motor nerve terminals confirmed previous reports of a significant loss of innervation at the NMJ in late-symptomatic (P24–P27) homozygous *Wst* mice, characterized by partially occupied and vacant endplates (Fig. 1). Partial occupancy of endplates by overlying motor nerve terminals is a morphological correlate associated with dying-back pathways, distinct from the rapid *in-situ* fragmentation occurring at the NMJ during WD (Miledi & Slater, 1970; Winlow & Usherwood, 1975; Fischer et al. 2004; Murray et al. 2008).

We extended these observations to include other muscle groups, finding evidence for similar synaptic pathology in the LAL muscle from the dorsal aspect of the head and flexor digitorum brevis muscle from the plantar aspect of the hind-paw (Fig. 2). In keeping with previous reports of a rostrocaudal progression of motor neuron degeneration in *Wst* mice, pathology was more severe in neurons supplying the LAL than those innervating the flexor digitorum brevis (cf. Fig. 2 in the current paper with Fig. 6 in Newbery et al. 2005). Closer examination of the distinct rostral and caudal bands of the LAL muscle, known to be differentially affected by dying-back pathology in mouse models of spinal muscular atrophy (SMA) (Murray et al. 2008), showed similar levels of synaptic pathology in each band (data not shown).

We next examined the ultrastructure of degenerating NMJs in late-symptomatic *Wst* mice (Fig. 1D and E). In all preparations examined (> 200 NMJs in total), we never observed any of the classical ultrastructural markers of WD (Miledi & Slater, 1970; Winlow & Usherwood, 1975). Motor nerve terminal plasma membranes remained intact, even during the process of retraction (as shown by partially occupied motor endplates; Fig. 1D and E). Similarly, nerve terminal organelles such as mitochondria and synaptic vesicles could clearly be identified and terminal Schwann cells were never observed engulfing or phagocytosing nerve terminals (Fig. 1D and E, and H and I). One other conspicuous morphological feature of *Wst* motor nerve terminals and distal axons was a conspicuous accumulation of neurofilaments (Fig. 1F–H), once again appearing very similar to previous reports of other dying-back neuropathies (Cifuentes-Diaz et al. 2002; Murray et al. 2008).

As mitochondrial fragmentation and synaptic vesicle depletion are two of the major hallmarks of WD (Miledi & Slater, 1970; Winlow & Usherwood, 1975), we undertook a more detailed ultrastructural investigation of these organelles. The vast majority of nerve terminal mitochondria remained intact (Fig. 1I) with the numbers of mitochondria displaying a disrupted morphology being consistently less than those previously described in normal 'healthy' nerve terminals (<10%; Winlow & Usherwood, 1975). Quantification of synaptic vesicle densities (see Materials and methods) revealed that, rather than vesicles being depleted in nerve terminals, the density of vesicles actually increased in *Wst* mice at both P20 and P26 (Fig. 1J). Thus, all of the morphological features of degeneration at the NMJ in *Wst* mice were characteristic of a retraction process more akin to dying-back pathology than classical WD.

As such an increase in synaptic vesicle numbers may imply altered synaptic function, we examined pre-synaptic function at the NMJ in late-symptomatic (P25) homozygous *Wst;YFP-H* mice using the vital styryl dye FM4–64 (see Materials and methods). The use of *Wst;YFP-H* mice allowed us to examine synaptic function at intact motor nerve terminals, indicated by the presence of YFP label (see below). As expected, all motor nerve terminals showed uptake of FM4–64 in LAL muscles from wild-type and heterozygous *Wst;YFP-H* littermate mice ($N = 4$ muscles). However, examples of intact motor nerve terminals with no FM4–64 uptake were observed in all LAL muscles from homozygous *Wst;YFP-H* mice ($N = 4$ muscles; Fig. 3). These data suggest that the presence of large numbers of synaptic vesicles in motor nerve terminals can be explained by the functional machinery required for exocytosis/endocytosis being impaired as part of the dying-back process in *Wst* mice. Thus, functional loss preceded morphological retraction, as previously reported for other dying-back neuropathies (Balice-Gordon et al. 2000; Pun et al. 2006).

Loss of *eEF1A2* expression triggers a dying-back neuropathy: axonal pathology

Although the disruption of NMJs was clearly an early pathological event in *Wst* mice, it remained unclear whether neuromuscular synapses and their distal axon collaterals were the initial site of neurodegeneration or whether proximal axonal degeneration back in the main peripheral nerve trunk was occurring concurrently or in advance. This remained a critical point to address as the classic criterion for a dying-back pathology defines a distal to proximal initiation and progression of pathology. To address this question, we cross-bred *Wst* mice with *thy1YFP-H* mice endogenously expressing YFP in a small subset of motor neurons (Feng et al. 2000). Homozygous *Wst;YFP-H* mice were phenotypically indistinguishable from non-YFP-expressing *Wst* mice, developing the same symptoms over the same time-course (data not shown).

Whole intercostal nerves supplying the transversus abdominis (which at the time-point examined showed signs of severe synaptic pathology) and tibial nerves supplying the lumbrical muscles (which at the time-point examined showed signs of more modest synaptic pathology) were dissected from late-symptomatic (P25) *Wst;YFP-H* mice

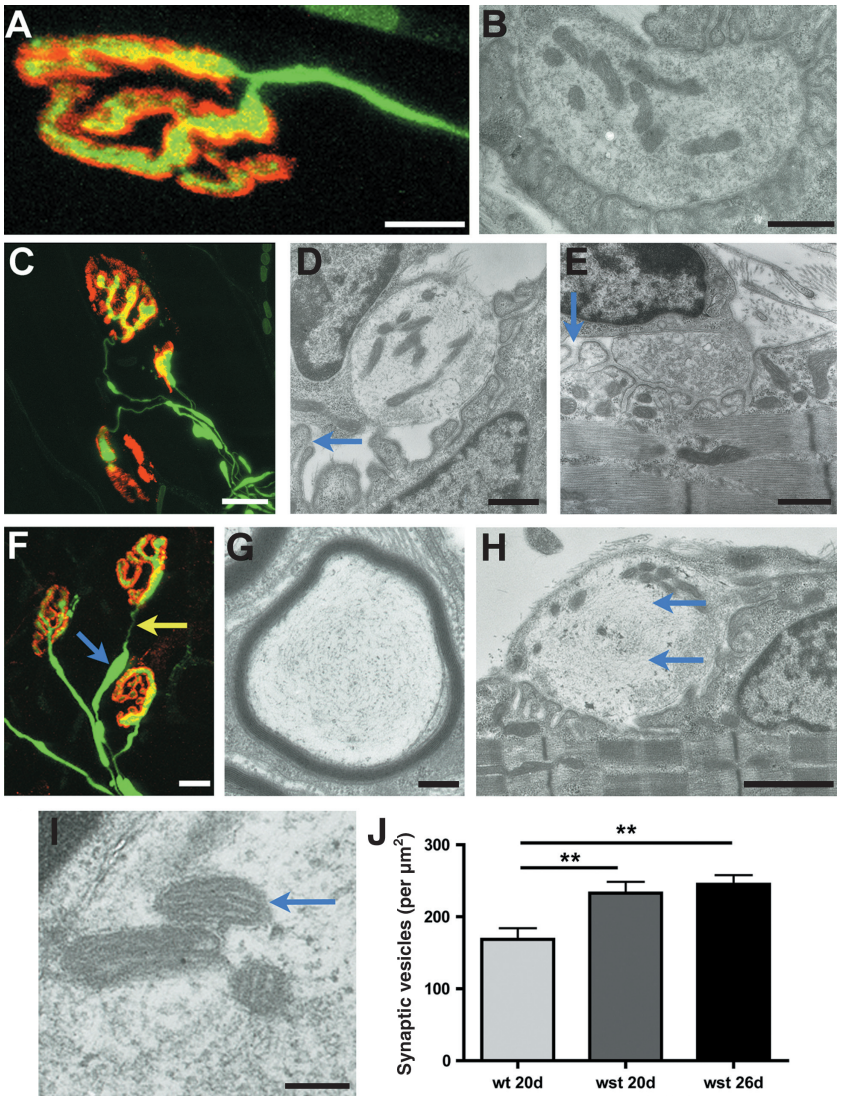

Fig. 1 Synaptic loss at the NMJ in *Wst* mice occurs by a pathway morphologically distinct from WD. (A) Confocal micrograph showing a normal, control NMJ in an immunohistochemically-labelled transversus abdominis (TVA) muscle preparation from a P21 wild-type littermate mouse [green, 165 kDa neurofilaments and SV2; red, post-synaptic acetylcholine receptors labelled with α-bungarotoxin conjugated to tetramethylrhodamine isothiocyanate (TRITC-α-bungarotoxin)]. (B) Electron micrograph showing a normal, control NMJ in a lumbrical muscle preparation from a P25 wild-type littermate mouse. (C) Confocal micrograph showing two partially occupied NMJs in an immunohistochemically-labelled TVA muscle preparation from a P21 *Wst* mouse (green, 165 kDa neurofilaments and SV2; red, post-synaptic acetylcholine receptors labelled with TRITC-α-bungarotoxin). Partial occupancy of endplates is a morphological characteristic associated with nerve terminal retraction (e.g. dying-back) processes rather than WD. Electron micrographs showing partially occupied NMJs (identified by regions of vacant post-synaptic folds; blue arrows) in the flexor digitorum brevis (D) and lumbrical (E) muscles from late-symptomatic (P25) *Wst* mice. Note how the remaining motor nerve terminal boutons show none of the characteristic ultrastructural signs of WD; mitochondria, synaptic vesicles and pre-synaptic plasma membranes were all present and intact, and there was no evidence of phagocytosis by the terminal Schwann cell. (F) Confocal micrograph showing characteristic neurofilament accumulation, alongside interspersed thinning, in distal axons (blue and yellow arrows respectively) and motor nerve terminals from a P25 *Wst* mouse lumbrical muscle. (G) Electron micrograph showing a cross-sectional profile of an axon from the intramuscular region of an intercostal nerve supplying the TVA muscle in a P26 *Wst* mouse. Note the presence of large neurofilament accumulations in the axonal cytoplasm (cf. F) and the absence of any degenerative characteristics; the myelin sheath and axonal membranes remain intact. (H) Electron micrograph showing a NMJ in the flexor digitorum brevis muscle from a P26 *Wst* mouse. Note the presence of large neurofilament accumulations in the motor nerve terminal (blue arrows) but the lack of any morphological characteristics of WD (see above). (I) High-power electron micrograph showing three mitochondria in a motor nerve terminal from the flexor digitorum brevis muscle of a P26 *Wst* mouse. Note how the mitochondrial membranes and cristae are preserved (disruption of mitochondrial morphology is one of the earliest signs of WD). (J) Bar chart (mean ± SEM) showing significant increases in synaptic vesicle densities in motor nerve terminals from the lumbrical muscles of *Wst* mice at P20 (early-symptomatic) and P26 (late-symptomatic) compared with wild-type littermates (**$P < 0.01$ for both ages, ANOVA with Tukey's post-hoc test; $N = 24$ nerve terminals and $n = 6694$ vesicles in P20 wild-type, $N = 20$ and $n = 3540$ in P20 *Wst*, $N = 26$ and $n = 8071$ in P26 *Wst*). Synaptic vesicles are normally depleted from motor nerve terminals during WD. Scale bars: 10 µm (A), 15 µm (C), 0.75 µm (B, D and E), 20 µm (F), 0.75 µm (G), 1 µm (H), 0.1 µm (I).

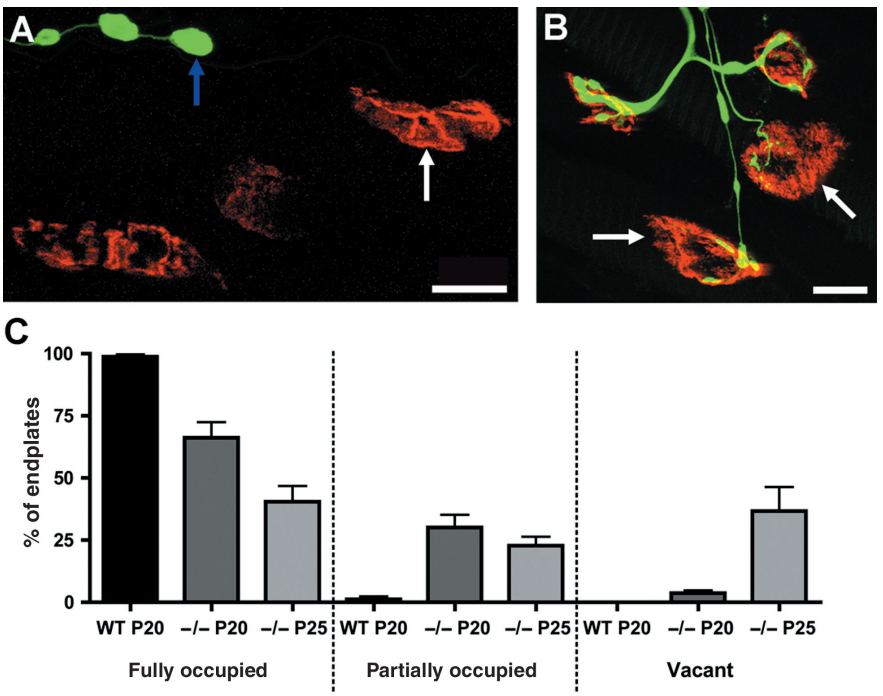

Fig. 2 Synaptic pathology extends to the flexor digitorum brevis (FDB) and levator auris longus (LAL) muscles in symptomatic *Wst* mice. Confocal micrographs showing NMJs in immunohistochemically-labelled LAL (A) and FDB (B) muscle preparations from P25 *Wst* mice (green, 165 kDa neurofilaments and SV2; red, post-synaptic acetylcholine receptors labelled with α-bungarotoxin conjugated to tetramethylrhodamine isothiocyanate). Partially occupied (white arrows in B) and vacant (white arrow in A) endplates were present throughout both muscle groups, as previously observed in transversus abdominis (TVA) and lumbrical muscles (Fig. 1 in the current paper; Newbery et al. 2005). Occasionally, remnants of synaptic terminals and distal axons withdrawing from post-synaptic endplates were observed ('retraction bulbs'; blue arrow in A). (C) Bar chart (mean ± SEM) showing the percentage of fully occupied endplates, partially occupied endplates and vacant endplates in LAL muscles from wild-type mice at P20 (WT P20; black bars; $N = 2$ mice), *Wst* mice at P20 (–/– P20; $N = 3$ mice) and *Wst* mice at P25 (–/– P25; $N = 4$ mice). Note how the percentage of fully occupied endplates declines and the percentage of vacant endplates increases with advancing age in *Wst* mice. Similar loss of pre-synaptic innervation was observed in FDB muscles at P25, albeit to a lesser extent than in LAL or TVA (as in neighbouring lumbrical muscles; ~30–40% of NMJs showed disrupted morphology; data not shown). Scale bars: 20 μm (A), 15 μm (B).

($N = 4$ intercostal nerves, $N = 4$ tibial nerves). Individual YFP-expressing axons were then imaged and reconstructed over a minimum distance of 1 mm (Fig. 4A and B). In all nerves examined, we never observed any signs of axonal degeneration. All individual YFP-labelled axons were intact along their entire length, with no evidence of axonal breaks, axon fragmentation or spheroid formation (Fig. 4A–C; cf. Beirowski et al. 2005). To confirm these observations, we also examined semi-thin toluidine-blue-stained sections of intercostal ($n = 11$ sections, $N = 4$ nerves) and tibial ($n = 10$ sections, $N = 2$ nerves) nerves from late-symptomatic P24 *Wst* mice (Fig. 4D). In all sections examined < 0.5% of axons were classified as having a 'degenerative' morphology (e.g. disrupted myelin sheath and/or axonal profile). Ultrastructural analyses of proximal and intramuscular axons from end-stage (P27) *Wst* mice again showed no evidence of gross axonal pathology (Fig. 4E). These data therefore reveal that synaptic loss occurs significantly in advance of axonal pathology in *Wst* mice, supporting the hypothesis that synaptic compartments of neurons are particularly sensitive to altered levels of *eEF1A2*.

Synapse loss occurs asynchronously within single motor units in *Wst* mice

As WD is known to bring about a relatively synchronous and rapid (i.e. within several hours) degeneration of NMJs (Miledi & Slater, 1970), whereas dying-back neuropathies are characterized by a progressive asynchronous loss of nerve terminals, we examined patterns of synaptic pathology occurring within the entire cohort of motor nerve terminals in single YFP-labelled motor units of *Wst*;*YFP-H* mice. We reconstructed and analysed synaptic cohorts of single motor units supplying LAL muscles from five late-symptomatic *Wst*;*YFP-H* mice (Fig. 5 and Supporting Information Fig. 1). Branching diagrams produced by tracing individual labelled motor units ($N = 5$) revealed a common response, with all motor neurons seemingly affected to a similar level (i.e. all motor units exhibited clear evidence of synaptic pathology). However, each motor unit displayed a heterogeneous range of synaptic morphologies, including intact synapses (fully occupied) and synapses at various stages of dismantling (partially occupied). Comparison of

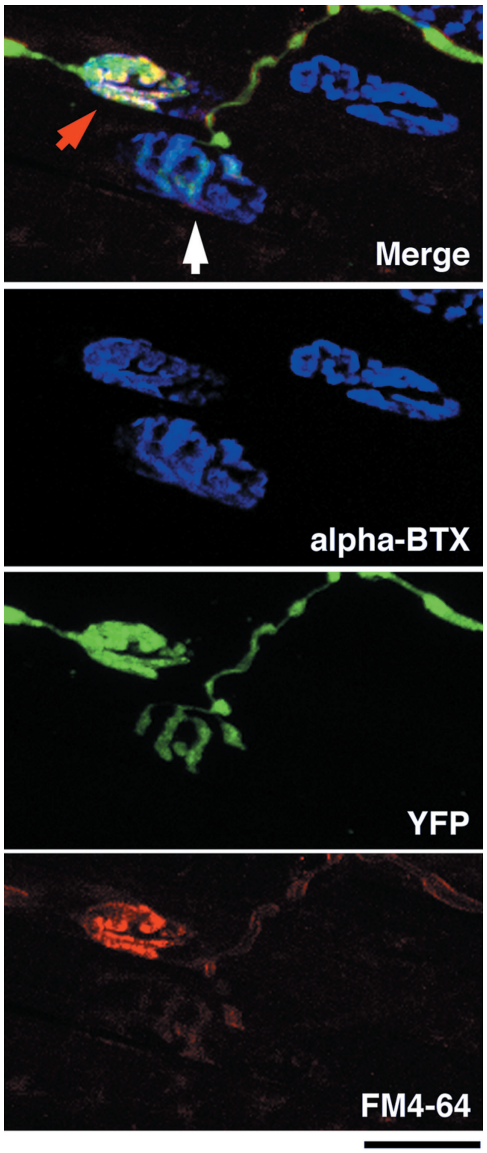

Fig. 3 Functional loss precedes structural loss at NMJs undergoing dying-back pathology in *Wst* mice. Confocal micrograph (merge of all three channels in top panel with separate channels shown below) of NMJs from a P25 *Wst;YFP-H* mouse LAL muscle. Motor nerve terminals were loaded with FM4–64FX using a depolarizing high-potassium solution leading to the selective labelling of functionally-active terminals (i.e. with the retained ability to recycle synaptic vesicles). In the preparation shown, two NMJs with motor nerve terminals containing YFP can be seen but only one of these motor nerve terminals demonstrated retained functional ability (red arrow; note the presence of strong FM4–64FX label in the bottom panel). The junction indicated by the white arrow was present morphologically (as shown by the YFP label) but had lost its functional capacity to recycle synaptic vesicles and hence had not taken up the FM4–64FX label. Thus, synaptic function was lost before morphological retraction occurred in *Wst* mice. By contrast, in control preparations from YFP-H wild-type littermates, all motor nerve terminals showed strong FM4–64FX labelling (data not shown). Scale bar, 35 μm.

the innervation states of neighbouring synapses that shared a single branch point showed that synapses were being lost progressively and asynchronously in *Wst* mice. This finding indicates that local mechanisms, resident at individual synapses, are likely to play an important role in determining an individual synapse's response to the effects of a loss of *eEF1A2*. Taken together with the other data presented above, these experiments demonstrate that disruption of *eEF1A2* in lower motor neurons and skeletal muscle fibres triggers dying-back pathways.

Molecular correlates of dying-back neuropathy in *Wst* mice: a role for ZPR1?

Although *eEF1A2*-specific mutations are not thought to be directly responsible for any human neurodegenerative conditions, the gene and its protein product share notable molecular linkages with other proteins known to be involved in the pathogenesis of other dying-back neuropathies such as the childhood motor neuron disease SMA. For example, eEF1A proteins assemble into complexes with the survival motor neuron protein (*SMN1*; where mutations abolish expression and cause SMA) and a zinc finger protein (*ZPR1*) (Gangwani et al. 1998; Mishra et al. 2007). Interestingly, the dying-back pathology observed following disruption of *eEF1A2* in *Wst* mice closely mirrors morphological correlates of lower motor neuron pathology occurring in mouse models of SMA and also in *ZPR1*-deficient mice (Monani et al. 2000, 2003; Doran et al. 2006; Murray et al. 2008). Therefore, we quantified levels of Smn protein in the spinal cord of late-symptomatic *Wst* mice (P25) and littermate controls using fluorescent (Li-COR) western blots to test whether the dying-back pathology in *Wst* mice could simply be accounted for by reduced levels of Smn protein resulting from decreased *eEF1A2* expression. Smn levels remained relatively stable in homozygous *Wst mice*, showing a slight trend towards increased rather than decreased expression levels (Fig. 6). This was in stark contrast to the significant reduction in Smn levels observed in the spinal cord of late-symptomatic *Smn–/–;SMN2* mice (an established mouse model of severe SMA) (Monani et al. 2000; Murray et al. 2008). Thus, the dying-back pathology observed in *Wst* mice could not be simply attributed to downstream changes in Smn protein levels. Next, we asked a similar question but this time focusing on levels of ZPR1 protein expression. Interestingly, ZPR1 protein levels were found to be consistently reduced in *Wst* mice, to a level similar to that found in *Smn–/–;SMN2* mice (Fig. 6). As reduced ZPR1 levels have been suggested to contribute to dying-back pathology in SMA (Gangwani et al. 2001; Helmken et al. 2003), a similar reduction in *Wst* mice may provide evidence for a common regulatory role of ZPR1 in regulating dying-back pathways in both *Wst* and *Smn–/–;SMN2* mice.

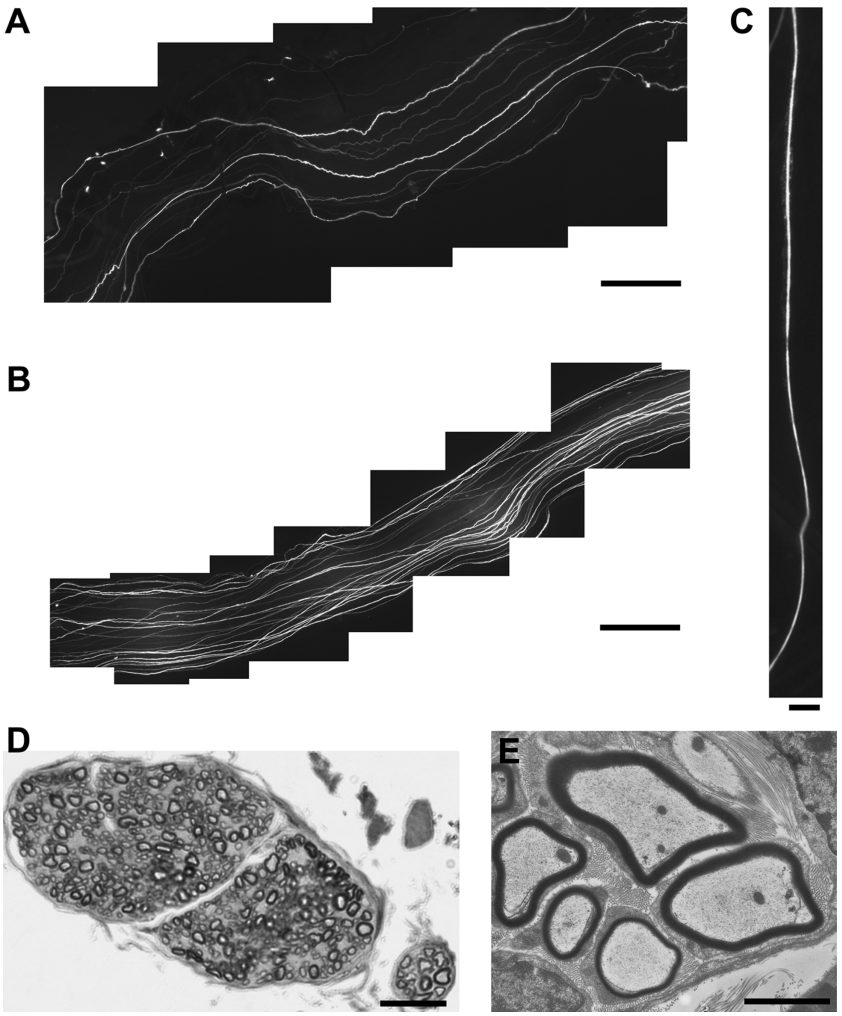

Fig. 4 Synaptic pathology occurs in the absence of axonal pathology in symptomatic *Wst* mice. Montage of fluorescence micrographs showing YFP-labelled axons in an intercostal nerve (A) (supplying the transversus abdominis muscle) and a tibial nerve (B) (supplying the lumbrical muscles) from P25 *Wst;YFP-H* mice. Note that not all axons are labelled with YFP, allowing direct visualization and tracing of individual axons for several hundred microns. All labelled axons were intact over the entire length reconstructed in both nerves. This is in stark contrast to the fragmented appearance of axons undergoing WD (cf. Beirowski et al. 2005). (C) High-power fluorescence micrograph of an individual YFP-labelled axon in an intercostal nerve from a P25 *Wst;YFP-H* mouse showing intact axonal morphology. (D) Cross-section of a toluidine blue-stained intercostal nerve from a P24 *Wst* mouse. Less than 1% of axons examined using this approach showed any morphological signs of degeneration. (E) Electron micrograph of axons from an intramuscular region of intercostal nerve from a P26 *Wst* mouse, supporting analysis of toluidine blue-stained sections (D) by showing no evidence of axonal degeneration. All axons examined had normal myelin sheaths and axonal membranes. Scale bars: 200 μm (A), 450 μm (B), 25 μm (C), 35 μm (D), 4 μm (E).

eEF1A2 is required for the normal initiation and progression of axotomy-induced WD

As we found strong evidence that *eEF1A2* is an important regulator of dying-back pathways *in vivo*, we next asked whether deficiencies in *eEF1A2* also exert any influence on WD pathways by studying responses to nerve injury in homozygous *Wst*, heterozygous *Wst* and wild-type littermate mice. For these experiments we examined lumbrical muscles as the synaptic pathology resulting from dying-back pathology was significantly less in these muscles compared with more rostral muscle groups (Figs 1 and 2) (Newbery et al. 2005), thereby minimizing the complexity of distinguishing disease-induced changes from those induced by nerve injury. Late-symptomatic (P24) *Wst* and *Wst;YFP-H* mice (as well as wild-type and heterozygous *Wst* littermates) were subjected to a unilateral tibial nerve cut under general anaesthesia. Following recovery and resumption of normal behaviour, mice were killed 24 h later (P25) and their lumbrical muscles and tibial nerves distal to the site of lesion were removed.

As expected, nerve lesion in wild-type littermate mice resulted in a complete loss of neuromuscular innervation at 24 h after surgery, via classical WD pathways characterized by rapid breakdown and fragmentation of pre-synaptic motor nerve terminals and distal axons (Fig. 7A and F). Surprisingly, the vast majority (~80%) of motor nerve terminals and their intramuscular axon collaterals remained intact in lumbrical muscles from homozygous *Wst* mice at 24 h after nerve lesion (Fig. 7B and F). Similarly, the tibial nerve distal to the site of nerve lesion showed no signs of degeneration in homozygous *Wst* mice assayed using YFP-H and ultrastructural techniques (Fig. 7C–E). As the tibial nerve is a mixed motor/sensory nerve, these experiments revealed that neither motor nor sensory axons showed signs of degeneration in homozygous *Wst* mice. Examination for early axonal ultrastructural indicators of WD (swelling and damage of mitochondria) (Miledi & Slater, 1970; Winlow & Usherwood, 1975) revealed subtle but widespread changes in wild-type nerves (~50% of axons examined showed mitochondrial changes or disruption of the myelin sheath; Fig. 7D) but the almost complete

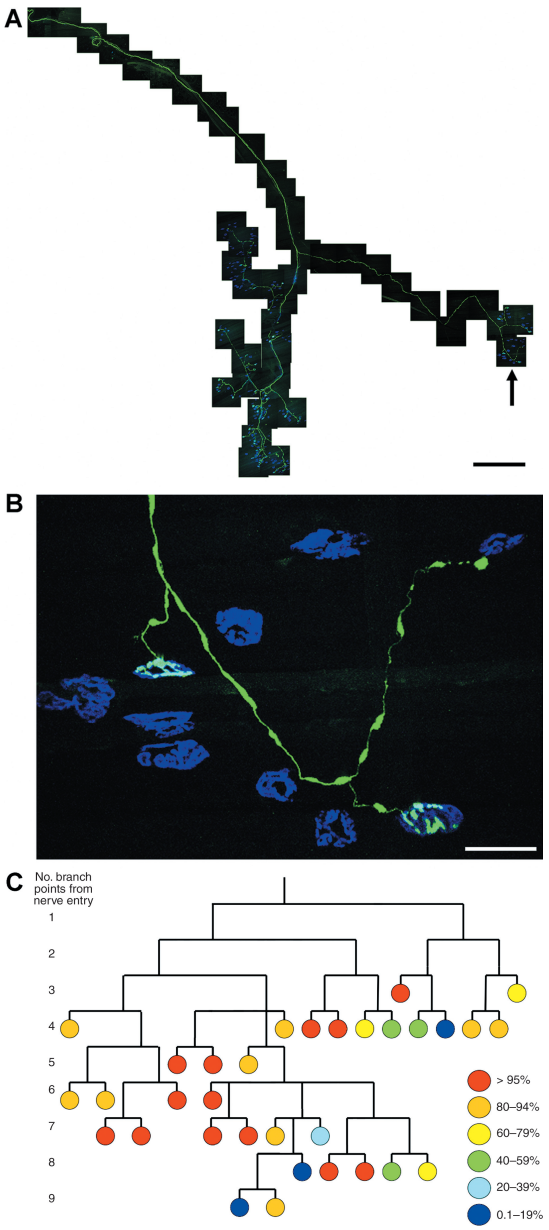

Fig. 5 Asynchronous loss of synapses at the NMJ within single motor units in late-symptomatic *Wst* mice. (A) Montage of confocal micrographs showing a single YFP-H-labelled motor unit from a P25 *Wst;YFP-H* mouse (green, YFP; blue, post-synaptic acetylcholine receptors labelled with α-bungarotoxin). (B) Higher power confocal micrograph showing a small region of the larger whole motor unit shown in A (position indicated by black arrow in A). Note how the first (far left) NMJ is fully occupied, the second (lower right) NMJ is partially occupied and the third (upper right) NMJ has lost its pre-synaptic input, remnants of which are left as a retraction bulb. (C) Branch diagram generated from an analysis of the single motor unit shown in A, with each individual NMJ represented as a circle relative to its branch point position within the motor unit. The occupancy status of each NMJ is represented by the colour of the circle (key to colours is on the right of the panel). Note how synaptic retraction occurred asynchronously throughout the motor unit, with a full spread of occupancies present. Note also how fully occupied (i.e. 'normal'; red) NMJs were distributed at locations throughout the motor unit, as were almost fully retracted NMJs (blue). Scale bars: 500 μm (A), 50 μm (B).

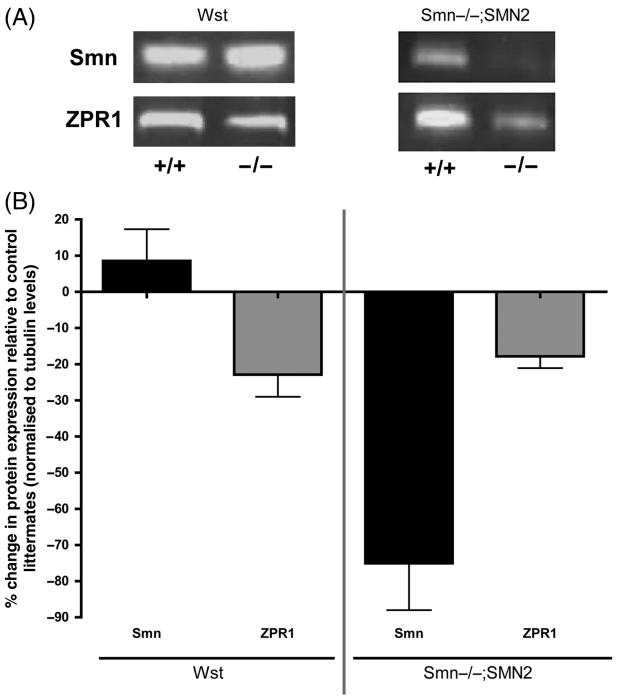

Fig. 6 Dying-back pathology in *Wst* mice occurs independently of changes in Smn protein expression but correlates with modest reductions in ZPR1 protein levels. (A) Representative fluorescent western blots showing levels of Smn and ZPR1 protein in *Wst* mice vs. control littermates (left panel) and *Smn–/–;SMN2* mice vs. control littermates (right panel). (B) Bar chart (mean ± SEM) showing expression levels of Smn and ZPR1 protein in the mid-thoracic spinal cord of late-symptomatic *Wst* (left bars; P25) and *Smn–/–;SMN2* (right bars; P5) mice compared with respective control littermate mice, quantified using fluorescent western blots ($N = 3$ mice per genotype). Smn protein levels did not decrease in *Wst* mice (if anything showing a modest increase in expression) but, as expected, decreased by around 75% in *Smn–/–;SMN2* mice. Thus, the dying-back pathology observed in *Wst* mice is not simply occurring due to reduced levels of Smn protein. ZPR1 protein levels, however, were reduced by similar amounts in both *Wst* and *Smn–/–;SMN2* mice.

absence of any early markers of WD in *Wst* nerves (only one out of ~200 axons showed signs of disrupted mitochondria; Fig. 7E). Importantly, we were able to rule out the possibility that the genetic background of the mice was influencing the WD process by comparing homozygous *Wst* mice with heterozygous and wild-type littermates (Fig. 7F).

In order to confirm that the significant inhibition of WD found in homozygous *Wst* mice extended beyond the 24 h period that we initially examined, we quantified degeneration in mice subjected to a unilateral tibial nerve cut at P23 followed by killing 48 h later (P25). Even at 48 h post-axotomy, approximately 50% of motor nerve terminals and their intramuscular axon collaterals remained intact in lumbrical muscles from homozygous *Wst* mice (Fig. 7G). This contrasts with the situation in wild-type and heterozygous littermates where almost all motor nerve terminals (> 95%) had undergone degeneration after 24 h (Fig. 7F).

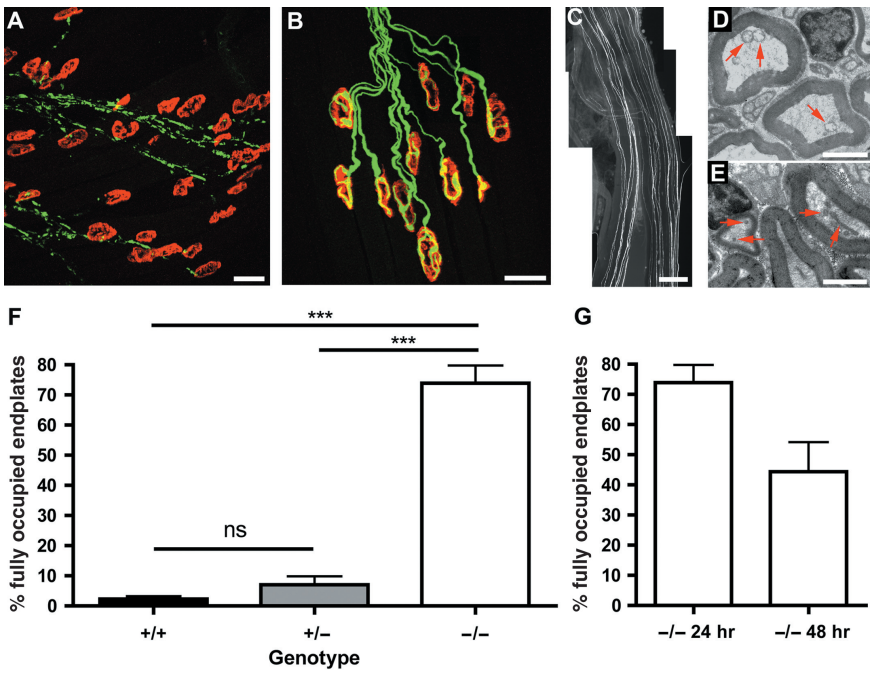

Fig. 7 *eEF1A2* expression is required for the normal initiation and progression of axotomy-induced WD. Confocal micrographs showing NMJs in immunohistochemically-labelled lumbrical muscle preparations from P25 wild-type (+/+) (A) and homozygous *Wst* (–/–) (B) mice at 24 h after a tibial nerve cut (green, 150 kDa neurofilaments; red, post-synaptic acetylcholine receptors). As expected, axotomy resulted in almost complete WD of motor nerve terminals and distal axon collaterals in lumbrical muscles of wild-type mice (A). Surprisingly, however, axotomy-induced WD was almost completely absent from homozygous *Wst* mice at the same time-point (B). (C) Montage of fluorescence micrographs showing YFP-labelled axons in a tibial nerve (supplying the lumbrical muscles) from a P25 *Wst;YFP-H* mouse at 24 h after a tibial nerve cut. Note the complete absence of any axonal pathology at this time-point. As expected, similar data were obtained from +/+ mice as gross morphological features of axonal WD do not begin to appear until 24 h after lesion (cf. Beirowski et al. 2005; data not shown). (D) Electron micrograph showing early ultrastructural signs of WD in +/+ tibial nerves at 24 h after axotomy (swollen and disrupted mitochondria; red arrows). (E) Electron micrograph showing lack of early ultrastructural signs of WD in –/– tibial nerves at 24 h after axotomy (mitochondria remained intact; red arrows). (F) Bar chart (mean ± SEM) showing the percentage of NMJs remaining in lumbrical muscles at 24 h post-axotomy (***$P < 0.001$; Kruskal Wallis test with Dunn's post-hoc; $n = 57$ muscles, $N = 19$ mice +/+; $n = 36$ muscles, $N = 12$ mice +/–; $n = 36$ muscles, $N = 12$ mice –/–). Note how < 5% of NMJs remained intact in muscles from wild-type mice, whereas ~80% of NMJs remained intact in muscles from homozygous *Wst* mice. (G) Bar chart (mean ± SEM) showing the percentage of NMJs remaining in lumbrical muscles from homozygous *Wst* mice at 24 and 48 h post-axotomy ($n = 36$ muscles, $N = 12$ mice –/– 24 h; $n = 6$ muscles, $N = 2$ mice –/– 48 h). Note how ~50% of NMJs remained intact in muscles from homozygous *Wst* mice even at 48 h post-axotomy. Scale bars: 50 μm (A and B), 200 μm (C), 2 μm (D and E).

It was not possible to extend the time-course of our investigations much beyond this 48 h period because the operated mice did not live beyond P26 (due to the severity of dying-back pathological changes in the more severely affected rostral muscle groups) and mice could not be operated earlier than P23 in order to ensure a complete loss of *eEF1A1* expression (cf. Pan et al. 2004). However, these experiments demonstrate that *eEF1A2* is required for the normal initiation and progression of WD. These data also further support the conclusion that the dying-back pathways instigated following disruption of *eEF1A2* in *Wst* mice are mechanistically distinct from WD, as WD pathways are actually inhibited (rather than triggered) in *Wst* mice.

Discussion

The experiments reported here raise four important conclusions. First, they demonstrate that the spontaneous loss of *eEF1A2* expression that occurs in *Wst* mutant mice triggers dying-back pathways in lower motor neurons *in vivo,* where synaptic loss at the NMJ is an early event. This supports the hypothesis that synaptic compartments of neurons are particularly sensitive to perturbations in neuronal homeostasis (Gillingwater & Ribchester, 2001; Wishart et al. 2006) and shows that *eEF1A2* expression is essential for the prevention of pre-synaptic degeneration *in vivo*. Second, they show that *eEF1A2* expression is required for the normal initiation and progression of WD following nerve injury *in vivo*. This finding adds significant support to previous experimental studies suggesting that WD is an active, genetically-regulated process, rather than a simple passive consequence of disconnection from the parent cell body (Mack et al. 2001; Coleman & Perry, 2002). Third, the experiments show that degeneration of axons and synapses can be regulated by at least two mechanistically-divergent pathways. Specifically, dying-back pathology can be caused by deficiencies in *eEF1A2*, whereas WD requires

eEF1A2 expression. This finding contradicts, to some extent, an emerging view that many axonal and synaptic degenerative pathways converge onto common underlying mechanisms (cf. Coleman, 2005). Fourth, they suggest that *eEF1A2*-dependent molecular cascades, potentially acting via ZPR1-dependent pathways, may be capable of modifying the type and/or severity of neurodegenerative pathways instigated in lower motor neurons. The current study therefore highlights the significant potential that exists for further investigations into the molecular pathways acting downstream of *eEF1A2* to provide novel insights into neurodegenerative cascades resident in axonal and synaptic compartments of lower motor neurons.

Can deficiencies in protein synthesis explain the neurodegenerative phenotype in *Wst* mice?

The most parsimonious explanation for the current findings is that defects in protein synthesis, resulting directly from a loss of *eEF1A2* expression and function, are responsible for triggering dying-back pathways and for the delay in WD. There is little doubt that deficiencies in *eEF1A* proteins lead to disruption of protein synthesis (Shultz et al. 1982; Chambers et al. 1998; Pan et al. 2004). Moreover, the protein synthesis machinery is known to influence axonal and synaptic form and function in neuronal cells (Piper & Holt, 2004; Grossman et al. 2006; McCann et al. 2007), and *eEF1A* is known to be important for local protein synthesis determining synaptic stability and function (Giustetto et al. 2003). However, although protein synthesis has been shown to influence neurodegeneration of axons and synapses *in vitro* (e.g. Stavisky et al. 2003), the influence of protein synthesis on neurodegenerative mechanisms resident in axons and synapses *in vivo* remains unclear.

It is not currently possible to directly visualize or measure *de-novo* protein synthesis in distal axonal and/or neuromuscular synaptic compartments with any accuracy, ruling out the possibility of definitively linking the induction of dying-back pathways to deficiencies in protein synthesis. Similarly, the current data do not allow us to directly link the inhibition of WD with deficiencies in local protein synthesis. However, *Wst* mice are likely to provide an ideal model system within which to further investigate downstream molecular mechanisms once more sensitive techniques to measure local neuronal protein synthesis become available. Its attraction as an experimental model is highlighted by the fact that *eEF1A2* deficiencies are restricted to neuronal cells and muscle, and are only instigated post-natally.

Could non-canonical roles of *eEF1A2* be responsible for the neurodegenerative phenotype in *Wst* mice?

Alternative hypotheses explaining the potential mechanisms underlying modifications in dying-back pathways and WD in *Wst* mice can be proposed in the light of other known non-canonical functions of *eEF1A* proteins. For example, several studies have implicated *eEF1A* proteins in assembly and stability of the cytoskeleton, including roles in actin binding and microtubule severing (Yang et al. 1990, 1993; Shiina et al. 1994). It is possible therefore that the dying-back pathways instigated in *Wst* mice occur as a direct result of perturbations in the stability of the axonal and synaptic cytoskeleton. Moreover, a loss of ability to transport the products of cytoskeletal disruption down the distal axon may explain the inhibition of WD pathways. If the latter were found to be true, it would provide experimental support for the hypothesis that WD is triggered by a signal that passes from the site of injury down to the nerve terminal (Miledi & Slater, 1970). Alternatively, it is possible that perturbations in synaptic plasticity pathways, known to be modulated by *eEF1A* levels (Giustetto et al. 2003), lead to destablilization of the NMJ and induction of dying-back pathology. However, it should be noted that it has yet to be demonstrated that the *eEF1A2* variant has the same non-canonical roles previously attributed to non-variant-specific *eEF1A* protein. It therefore also remains possible that *eEF1A2* has as yet unidentified roles that are responsible for the phenotypes described in the current study.

It should also be noted that it is by no means certain that the same downstream effects resulting from loss of *eEF1A2* in *Wst* mice are responsible for the dual effects on dying-back pathways and WD pathways. Further mechanistic experiments, beyond the scope of the current study, are required to distinguish the specific characteristics or molecular targets of *eEF1A2* required to prevent a dying-back neuropathy and/or inhibit the initiation and progression of WD.

Implications for the stability and vulnerability of lower motor neurons in human motor neuron disease

Although *eEF1A2* mutations are not currently thought to be directly responsible for any human neurodegenerative conditions, the gene and its protein product are known to interact with other proteins that regulate dying-back pathology in human neurodegenerative conditions such as the childhood motor neuron disease SMA. eEF1A proteins assemble into complexes with the survival motor neuron protein (*SMN1*; mutations in which cause SMA) and a zinc finger protein (*ZPR1*) (Gangwani et al. 1998; Mishra et al. 2007). The finding that dying-back pathology occurring in *Wst* mice closely resembles lower motor neuron pathology occurring in mouse models of SMA and in *ZPR1*-deficient mice (Monani et al. 2000, 2003; Doran et al. 2006; Murray et al. 2008) prompted us to examine whether the pathways modified by loss *of eEF1A2* converged onto those involving SMN and ZPR1. We found that dying-back pathology in *Wst* mice cannot be attributed to corresponding reductions in Smn protein levels, suggesting

that dying-back pathology in *Wst* and *Smn–/–;SMN2* mice is not triggered by the same molecular cues. However, our observation that ZPR1 protein levels were modestly reduced in *Wst* mice, to a level similar to that found in *Smn–/–;SMN2* mice, raises the possibility of shared downstream mechanistic pathways focused around ZPR1. As decreasing ZPR1 levels have been shown to correlate with disease severity in SMA patients (Helmken et al. 2003) and ZPR1 is known to be required for the normal maintenance and localization of Smn protein (Gangwani et al. 2001), it is tempting to speculate that ZPR1 is capable of playing an important role in regulating lower motor neuron vulnerability in SMA and in *Wst* mice. Further investigations into the expression and function of *ZPR1* in *Wst* and *Smn–/–;SMN2* mice may therefore provide novel insights into cellular and molecular cascades regulating the vulnerability of motor neurons in disease. Moreover, as the current data suggest that *eEF1A2* is required to prevent pre-synaptic degeneration via a dying-back neuropathy, it may also be worth investigating the possibility of increasing levels of *eEF1A2*, on its own or in combination with ZPR1, as a potential neuroprotective strategy in dying-back neuropathies, such as SMA.

Conclusions

In this study we have shown that loss of expression of the translation elongation factor *eEF1A2* triggers a dying-back neuropathy characterized by early loss of motor nerve terminals at the NMJ. In sharp contrast, in the same motor neurons the process of WD was significantly delayed following an experimental nerve lesion. This suggests that dying-back pathology and WD are regulated by fundamentally different mechanisms *in vivo*.

Acknowledgements

We thank Dr S. Parson, Dr C. Abbott, Dr H. Newbery, T. Chater and members of the laboratory of T.H.G. for helpful assistance with and advice on this study. This study was supported by grants to T.H.G. from Medical Research Scotland, BDF Newlife and the Anatomical Society of Great Britain and Ireland. L.M.M. is the recipient of a PhD Studentship from the Anatomical Society of Great Britain and Ireland.

References

Balice-Gordon RJ, Smith DB, Goldman J, et al. (2000) Functional motor unit failure precedes neuromuscular degeneration in canine motor neuron disease. *Ann Neurol* **47**, 596–605.

Baxter B, Gillingwater TH, Parson SH (2008) Rapid loss of motor nerve terminals following hypoxia-reperfusion injury occurs via mechanisms distinct from classic Wallerian degeneration. *J Anat* **212**, 827–835.

Beirowski B, Adalbert R, Wagner D, et al. (2005) The progressive nature of Wallerian degeneration in wild-type and slow Wallerian degeneration (WldS) nerves. *BMC Neurosci* **6**(1), 6.

Bettini NL, Moores TS, Baxter B, Deuchars J, Parson SH (2007) Dynamic remodelling of synapses can occur in the absence of the parent cell body. *BMC Neurosci* **8**, 79.

Chambers DM, Peters J, Abbott CM (1998) The lethal mutation of the mouse wasted (wst) is a deletion that abolishes expression of a tissue-specific isoform of translation elongation factor 1alpha, encoded by the Eef1a2 gene. *Proc Natl Acad Sci USA* **95**, 4463–4468.

Cifuentes-Diaz C, Nicole S, Velasco ME, et al. (2002) Neurofilament accumulation at the motor endplate and lack of axonal sprouting in a spinal muscular atrophy mouse model. *Hum Mol Genet* **11**, 1439–1447.

Coleman M (2005) Axon degeneration mechanisms: commonality amid diversity. *Nat Rev Neurosci* **6**, 889–898.

Coleman MP, Perry VH (2002) Axon pathology in neurological disease: a neglected therapeutic target. *Trends Neurosci* **25**, 532–537.

Condeelis J (1995) Elongation factor 1 alpha, translation and the cytoskeleton. *Trends Biochem Sci* **20**, 169–170.

Doran B, Gherbesi N, Hendricks G, Flavell RA, Davis RJ, Gangwani L (2006) Deficiency of the zinc finger protein ZPR1 causes neurodegeneration. *Proc Natl Acad Sci USA* **103**, 7471–7475.

Feng G, Mellor RH, Bernstein M, et al. (2000) Imaging neuronal subsets in transgenic mice expressing multiple spectral variants of GFP. *Neuron* **28**, 41–51.

Ferguson B, Matyszak MK, Esiri MM, Perry VH (1997) Axonal damage in acute multiple sclerosis lesions. *Brain* **120**, 393–399.

Fischer LR, Culver DG, Tennant P, et al. (2004) Amyotrophic lateral sclerosis is a distal axonopathy in mice and man. *Exp Neurol* **185**, 232–240.

Frey D, Schneider C, Xu L, Borg J, Spooren W, Caroni P (2000) Early and selective loss of neuromuscular synapse subtypes with low sprouting competence in motoneuron diseases. *J Neurosci* **20**, 2534–2542.

Gangwani L, Mikrut M, Galcheva-Gargova Z, Davis RJ (1998) Interaction of ZPR1 with translation elongation factor-1alpha in proliferating cells. *J Cell Biol* **143**, 1471–1484.

Gangwani L, Mikrut M, Theroux S, Sharma M, Davis RJ (2001) Spinal muscular atrophy disrupts the interaction of ZPR1 with the SMN protein. *Nat Cell Biol* **3**, 376–383.

Gillingwater TH, Ingham CA, Coleman MP, Ribchester RR (2003) Ultrastructural correlates of synapse withdrawal at axotomised neuromuscular junctions in mutant and transgenic mice expressing the Wld gene. *J Anat* **203**, 265–276.

Gillingwater TH, Ribchester RR (2001) Compartmental neurodegeneration and synaptic plasticity in the Wlds mutant mouse. *J Physiol* **534**, 627–639.

Gillingwater TH, Ribchester RR (2003) The relationship of neuromuscular synapse elimination to synaptic degeneration and pathology: Insights from Wlds and other mutant mice. *J Neurocytol* **32**, 863–881.

Gillingwater TH, Ingham CA, Parry KE, et al. (2006) Delayed synaptic degeneration in the CNS of Wlds mice after cortical lesion. *Brain* **129**, 1546–1556.

Giustetto M, Hegde AN, Si K, et al. (2003) Axonal transport of eukaryotic translation elongation factor 1alpha mRNA couples transcription in the nucleus to long-term facilitation at the synapse. *Proc Natl Acad Sci USA* **100**, 13680–13685.

Grossman AW, Aldridge GM, Weiler IJ, Greenough WT (2006) Local protein synthesis and spine morphogenesis: Fragile X syndrome and beyond. *J Neurosci* **26**, 7151–7155.

Helmken C, Hofmann Y, Schoenen F, et al. (2003) Evidence for a modifying pathway in SMA discordant families: reduced SMN

level decreases the amount of its interacting partners and Htra2-beta1. *Hum Genet* **114**, 11–21.

Hoopfer ED, McLaughlin T, Watts RJ, Schuldiner O, O'Leary DDM, Luo L (2006) Wlds protection distinguishes axon degeneration following injury from naturally occurring developmental pruning. *Neuron* **50**, 883–895.

Keswani SC, Jack C, Zhou C, Hoke A (2006) Establishment of a rodent model of HIV-associated sensory neuropathy. *J Neurosci* **26**, 10299–10304.

Khalyfa A, Bourbeau D, Chen E, et al. (2001) Characterization of elongation factor-1A (eEF1A-1) and eEF1A-2/S1 protein expression in normal and wasted mice. *J Biol Chem* **276**, 22915–22922.

Mack TGA, Reiner M, Beirowski B, et al. (2001) Wallerian degeneration of injured axons and synapses is delayed by a Ube4b/Nmnat chimeric gene. *Nat Neurosci* **4**, 1199–1206.

McCann CM, Nguyen QT, Santo Neto H, Lichtman JW (2007) Rapid synapse elimination after postsynaptic protein synthesis inhibition in vivo. *J Neurosci* **27**, 6064–6067.

Mi W, Beirowski B, Gillingwater TH, et al. (2005) The slow Wallerian degeneration gene, *WldS*, inhibits axonal spheroid pathology in gracile axonal dystrophy mice. *Brain* **128**, 405–416.

Miledi R, Slater CR (1970) On the degeneration of rat neuromuscular junctions after nerve section. *J Physiol* **207**, 507–528.

Mishra AK, Gangwani L, Davis RJ, Lambright DG (2007) Structural insights into the interaction of the evolutionarily conserved ZPR1 domain tandem with eukaryotic EF1A, receptors, and SMN complexes. *Proc Natl Acad Sci USA* **104**, 13930–13935.

Monani UR, Pastore MT, Gavrilina TO, et al. (2003) A transgene carrying an A2G missense mutation in the SMN gene modulates phenotypic severity in mice with severe (type I) spinal muscular atrophy. *J Cell Biol* **160**, 41–52.

Monani UR, Sendtner M, Coovert DD, et al. (2000) The human centromeric survival motor neuron gene (SMN2) rescues embryonic lethality in Smn(–/–) mice and results in a mouse with spinal muscular atrophy. *Hum Mol Genet* **9**, 333–339.

Murray LM, Comley LH, Thomson D, Parkinson N, Talbot K, Gillingwater TH (2008) Selective vulnerability of motor neurons and dissociation of pre- and post-synaptic pathology at the neuromuscular junction in mouse models of spinal muscular atrophy. *Hum Mol Genet* **17**, 949–962.

Newbery HJ, Gillingwater TH, Dharmasaroja P, et al. (2005) Progressive loss of motor neuron function in *Wasted* mice: Effects of a spontaneous null mutation in the gene for the eEF1A2 translation factor. *J Neuropathol Exp Neurol* **64**, 295–303.

Newbery HJ, Loh DH, O'Donoghue JE, et al. (2007) Translation elongation factor eEF1A2 is essential for post-weaning survival in mice. *J Biol Chem* **282**, 28951–28959.

Pan J, Ruest LB, Xu S, Wang E (2004) Immuno-characterization of the switch of peptide elongation factors eEF1A-1/EF-1alpha and eEF1A-2/S1 in the central nervous system during mouse development. *Brain Res Dev Brain Res* **149**, 1–8.

Perry VH, Anthony DC (1999) Axon damage and repair in multiple sclerosis. *Philos Trans R Soc Lond B Biol Sci* **354**, 1641–1647.

Piper M, Holt C (2004) RNA translation in axons. *Annu Rev Cell Dev Biol* **20**, 505–523.

Pun S, Santos AF, Saxena S, Xu L, Caroni P (2006) Selective vulnerability and pruning of phasic motoneuron axons in motoneuron disease alleviated by CNTF. *Nat Neurosci* **9**, 408–419.

Saxena S, Caroni P (2007) Mechanisms of axon degeneration: from development to disease. *Prog Neurobiol* **83**, 174–191.

Schmalbruch H, Jensen HJ, Bjaerg M, Kamieniecka Z, Kurland L (1991) A new mouse mutant with progressive motor neuronopathy. *J Neuropathol Exp Neurol* **50**, 192–204.

Shamovsky I, Ivannikov M, Kandel ES, Gershon D, Nudler E (2006) RNA-mediated response to heat shock in mammalian cells. *Nature* **440**, 556–560.

Shiina N, Gotoh Y, Kubomura N, Iwamatsu A, Nishida E (1994) Microtubule severing by elongation factor 1 alpha. *Science* **266**, 282–285.

Shultz LD, Sweet HO, Davisson MT, Coman DR (1982) 'Wasted', a new mutant of the mouse with abnormalities characteristic to ataxia telangiectasia. *Nature* **297**, 402–404.

Stavisky RC, Britt JM, Zuzek A, Pham T, Marzullo TC, Bittner GD (2003) Degeneration of mammalian PNS and CNS axons is accelerated by incubation with protein synthesis inhibitors. *Neurosci Res* **47**, 445–449.

Winlow W, Usherwood PN (1975) Ultrastructural studies of normal and degenerating mouse neuromuscular junctions. *J Neurocytol* **4**, 377–394.

Wishart TM, Parson SH, Gillingwater TH (2006) Synaptic vulnerability in neurodegenerative disease. *J Neuropathol Exp Neurol* **65**, 733–739.

Wishart TM, Paterson JM, Short DM, et al. (2007) Differential proteomics analysis of synaptic proteins identifies potential cellular targets and protein mediators of synaptic neuroprotection conferred by the slow Wallerian degeneration (*Wlds*) gene. *Mol Cell Proteomics* **6**, 1318–1330.

Yang F, Demma M, Warren V, Dharmawardhane S, Condeelis J (1990) Identification of an actin-binding protein from Dictyostelium as elongation factor 1a. *Nature* **347**, 494–496.

Yang W, Burkhart W, Cavallius J, Merrick WC, Boss WF (1993) Purification and characterization of a phosphatidylinositol 4-kinase activator in carrot cells. *J Biol Chem* **268**, 392–398.

Supporting information

Additional Supporting Information may be found in the online version of this article:

Fig. S1 Additional branch diagram reconstructions of single motor units undergoing dying-back pathology in homozygous *Wst* mice.

Please note: Wiley-Blackwell are not responsible for the content or functionality of any supporting materials supplied by the authors. Any queries (other than missing material) should be directed to the corresponding author for the article.